Gradient Induced Motion Control of Drifting Solitary Structures in a Nonlinear Optical Single Feedback Experiment

Carsten Cleff, Björn Gütlich, and Cornelia Denz

Institut für Angewandte Physik, and Center for Nonlinear Science, Westfälische Wilhelms–Universität Münster, Corrensstraße 2-4, 48149 Münster, Germany

(Received 8 October 2007; published 13 June 2008)

We realize an absolute position control of drifting dissipative optical solitons by injecting an incoherent amplitude parameter gradient onto the nonlinear optical system. This allows for two-dimensional, arbitrary control patterns. The control of the soliton drift velocity is studied applying a periodic, hexagonally shaped modulation. The guiding of dissipative solitons by one- and two-dimensional parameter modulations is demonstrated. Furthermore, one-dimensional, line-shaped parameter modulations are designed to act as barriers for dissipative solitons, allowing implementations of position selectors for solitons. The interaction of dissipative optical solitons with barriers is studied for different barrier parameters.

DOI: 10.1103/PhysRevLett.100.233902 PACS numbers: 42.65.Pc, 42.65.Tg

Dissipative solitons exist in a number of bistable nonlinear systems driven far from equilibrium [1]. They represent localized nonlinear objects with a robust spatial shape based on self-organized spontaneous formation. Particularly, in optical systems, dissipative solitons have been observed in active as well as passive optical cavities, and in nonlinear single mirror feedback systems [2–5], often named as solitary structures.

The bistability allows dissipative solitons to be switched on and off on a homogeneous background, thus having binary features. Because of this, dissipative solitons are considered as an optical bit for image processing using nonlinear optics. Applications ranging from routing and switching of optical data to all-optical data storage have been suggested [2]. It is of importance for these applications that dissipative solitons can move in phase gradients due to a spatial symmetry breaking [6,7]. Out of this reason, dissipative optical solitons are also influenced by high-frequency spatial parameter gradients induced by inhomogeneities of the optical system, resulting in an irregular motion and mutual interactions of the solitons and thereby challenging applications.

In the past, relative distances between optical dissipative solitons as well as the symmetry of their arrangements have been controlled successfully with different approaches in Fourier space [8,9]. However, these methods do not provide the possibility of an absolute position control of dissipative optical solitons in real space. This can only be realized by imposing an external parameter gradient onto the nonlinear system [6,10–14]. In this Letter, we propose and demonstrate a different approach to external position control based on an incoherent amplitude control. This allows for two-dimensional, arbitrary control patterns. With this technique, it is possible to control velocity, direction of motion, and absolute position of dissipative solitary structures. Moreover, the use of line-shaped modulations allows creating barriers to implement a position selector for dissipative solitons.

The potential of this technique is demonstrated exemplarily in a nonlinear optical single feedback system with a liquid crystal light valve (LCLV) as nonlinearity. In particular, we study the interaction and motion control of dissipative optical solitons drifting at constant velocity in one direction with different static parameter modulations.

A scheme of the experimental LCLV single feedback system is shown in Fig. 1. The reflective LCLV consists of a liquid crystal layer, a dielectric mirror, and a photoconductive layer sandwiched between transparent electrodes, and provides a saturable Kerr nonlinearity. The expanded planar pump wave incident on the liquid crystal layer, polarized 45° with respect to the LCLV's optical axis, is reflected internally and leaves the LCLV modulated in phase and polarization state. After a virtual free space propagation ($L = -15$ cm), the wave again passes a polarizer [15]. Diffraction converts the initial phase modulation into an intensity distribution during propagation. The resulting intensity distribution is imaged onto the photoconductive layer, thereby closing the feedback loop. A dove prism corrects rotational misalignments. A partial reflection at beam splitter (BS2) is used to monitor the optical far and near field with a CCD camera.

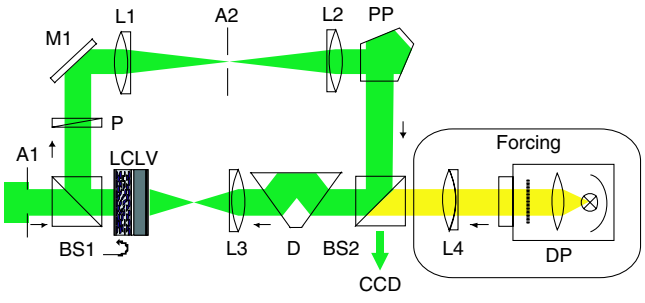

FIG. 1 (color online). Sketch of the LCLV single feedback system with external control. A: aperture; BS: beam splitter; P: polarizer; M: mirror; L: lens; PP: penta prism; D: dove prism; DP: data projector; CCD: camera.

Above a threshold of the laser pump intensity, the uniform planar wave solution becomes unstable, and the system exhibits self-organized pattern formation [15]. If the polarizer is set to an angle of $-45°$ with respect to the LCLV's optical axis, bistability between a uniform dark solution and a patterned bright solution is provided, allowing bright solitary structures to be formed spontaneously [5].

The external incoherent amplitude control is realized by injecting light from a data projector into the system. It is imaged to the photoconductor of the LCLV, where intensity gradients are converted into phase gradients, thus enabling motion control of solitary structures [13]. The projector provides a gray scale resolution of 8 bit to change the control strength. A single gray scale level equals 1.5% of the homogeneous background in the feedback loop, whereas the intensity of a solitary structure is one magnitude higher. Video sequences are used as control signals. The sequences display the control distribution only during the first second of operation. During the next second, solitary structures are ignited by locally increasing the control to the maximum gray scale level (255 gs). Subsequently, the addressing signal is turned off, and it is only the control distribution that remains.

If solitary structures are ignited in the system without drift, they experience a strong influence of spatial LCLV inhomogeneities on their behavior [9]. Favored addressing positions and a slow spontaneous drift of the solitary structures can be observed. In order to realize moving solitary structures, the influence of nonuniformities on the drift motion has to be controlled.

First, we induce a constant drift motion in one direction by detuning one of the feedback mirrors, thereby establishing a linear phase gradient. Fifty solitary structures are addressed at five positions in sequence, and the motion without an external control signal is monitored. The superposition of the resulting trajectories is shown in Fig. 2. Inhomogeneities lead to a development of predefined routes for drifting solitary structures. As previously demonstrated in steady state [12], external amplitude control enables balancing of these inhomogeneities.

In order to realize an absolute position control in real space, we first demonstrate the possibility of modulating the drift velocity. A periodic, hexagonally shaped control signal [Fig. 3(a)] with wave numbers varying between $k = 5.4\ \mathrm{mm}^{-1}$ and $k = 14.4\ \mathrm{mm}^{-1}$ is implemented. The control induces a periodic modulation of the drift velocity [Fig. 3(b)]. In correspondence to the control signal, a sine fit matches with the experimental data. Its noise characteristics are strongly related to the width of the first order self-diffraction ring of the solitary structures in Fourier space, which is found to be $k_s = 10.1\ \mathrm{mm}^{-1}$. When the wave number k is higher than k_s, noise increases due to the fact that a solitary structure is affected by more than one grid point. Above $k = 14.4\ \mathrm{mm}^{-1}$ the noise becomes strong enough to obscure the modulation. In the parameter region $k = 5.4$–$14.4\ \mathrm{mm}^{-1}$, we observe a linear dependence of the frequency of the velocity modulation f on the wave number of the grid, k (Fig. 4), indicating a reliable control of the drift velocity.

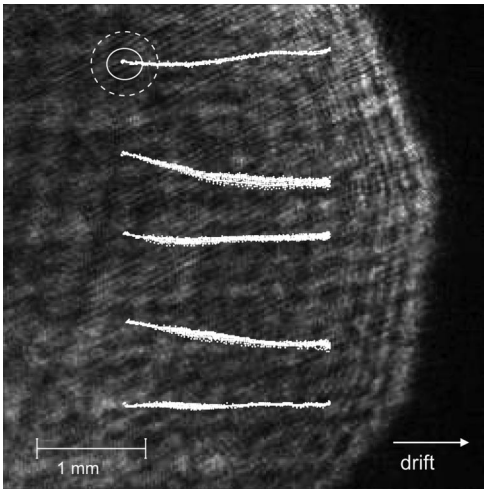

FIG. 2. Inhomogeneities induce predefined solitary structure paths. The figure shows the superposition of 50 trajectories of drifting solitary structures at each position addressed.

To enable the guiding of solitary structures, one-dimensional, line-shaped intensity distributions are used with a defined gray scale modulation [Fig. 5(a)]. On a background of a gray scale level of 80 gs, a line of 120 gs is inserted adjacent to dark lines of 0 gs. Thereby different gradients are achieved between background and the bright and dark lines. The lines have a width of 0.4 mm. The contrast of the induced phase modulation relative to the background is about 25%. However, it decreases rapidly due to the phase-amplitude transformation during free space propagation in the system. Therefore, the control signal is only weakly visible at the position of the CCD camera. The drift direction [marked in Fig. 5(a)] is oriented at 45° with respect to the line structure. Two solitary structures are ignited in different conditions on the LCLV transverse plane as shown in Fig. 5. One solitary structure is ignited on the bright center of the line structure, the other

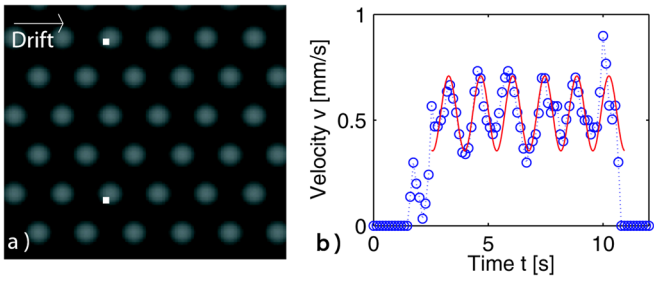

FIG. 3 (color online). (a) Periodic, hexagonal control signal with $k = 7.2\ \mathrm{mm}^{-1}$. (b) Resulting periodic modulation of the velocity of a solitary structure.

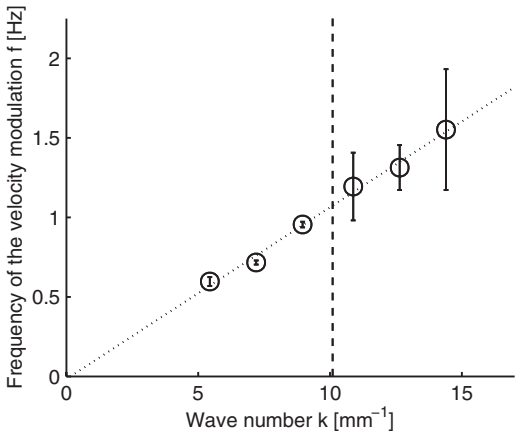

FIG. 4. The frequency of the velocity profile f depends linearly on the wave number k of the control signal. The dashed line marks the wave number k_s of the first order self-diffraction ring of a solitary structure in Fourier space.

one on the homogeneous background. The solitary structure ignited on the background moves parallel to the drift direction, whereas the one ignited at the line structure is guided parallel to the line structure in the vertical direction [Fig. 5(b)]. Both propagate on the transverse plane with the same velocity in the vertical direction. Figure 5(b) depicts the motion of the guided solitary structure, stopped by inhomogeneities. Because of the gradient difference chosen, the freely drifting one can enter the line structure and is guided as well.

These outstanding guiding properties can be easily extended to more complex line-shaped patterns. In Fig. 6(a) a control signal in the form of a staircase is illustrated. The trajectory of the guided solitary structure is depicted in Fig. 6(b). The motion of the solitary structure clearly follows the staircase. In the central part, inhomogeneities cause a defect, and therefore the solitary structure does not perfectly follow the predefined control path.

Targeting potential applications of solitary structures such as all-optical routing of data, we also created an intensity distribution that allows blocking of drifting soli-

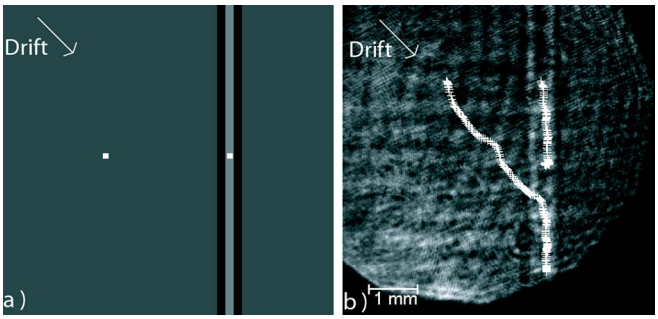

FIG. 5 (color online). (a) Line structure geometry for control signal to guide solitary structures. (b) One solitary structure is guided from the start and stopped by inhomogeneities. Another one moves on the line structure and is guided as well.

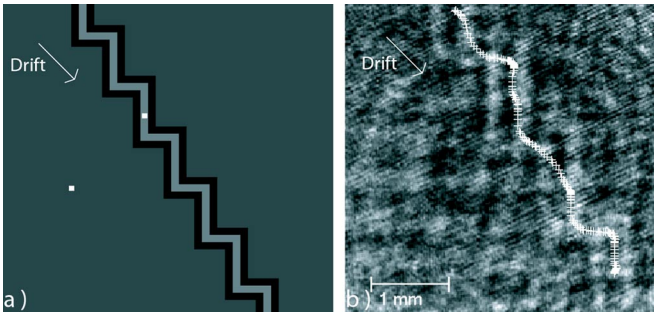

FIG. 6 (color online). (a) Staircase control signal for two-dimensional guiding. (b) The solitary structure's motion follows the staircase.

tary structures at specific spatial positions. An appropriate barrier consists of a dark one-dimensional line with a gray scale level of 0 gs. Because the intensity of the control is changed compared to the previous implementations, one gray scale now equals 1.2% of the background intensity in the feedback loop. Therefore, solitary structures can no longer exist in the dark domain. Adjacent domains of higher gray scale level (120 gs) increase the gradient, allowing solitary structures with a drift velocity up to $v \approx 0.33$ mm/s by gradient force to stop. Figure 7(a) shows a control scheme that allows solitary structures to pass only at a gap. The gap size is comparable to the soliton size. Solitary structures are ignited at a distance of 0.62 mm from the barrier at different transverse positions relative to the gap in the barrier. This distance equals the size of the first order self-diffraction ring of a solitary structure. The drift direction is perpendicular to the barrier and the drift velocity is $v = 0.5$ mm/s. Trajectories of the solitary structures are depicted in Fig. 7(b). Those ignited at the horizontal position of the gap are able to pass the barrier. All other ones disappear colliding with the barrier. To gain insight into the interaction of solitary structures with this kind of barriers, more detailed experiments were performed. We investigated the behavior of solitary structures for interaction with the barrier and its edge. For this reason, a control signal representing a half-barrier is created [Fig. 8(a)]. The barrier has the same geometry as above,

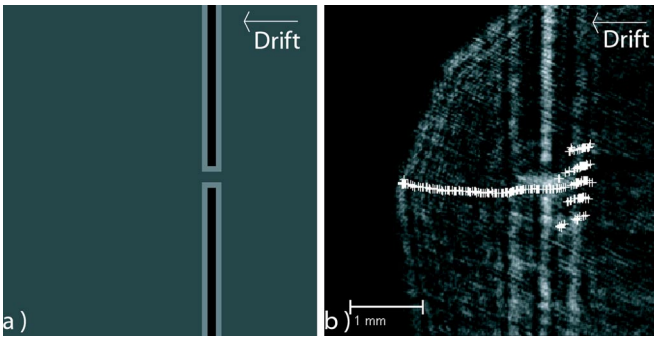

FIG. 7 (color online). (a) A control signal with two barriers (b) selects solitary structures depending on their spatial position.

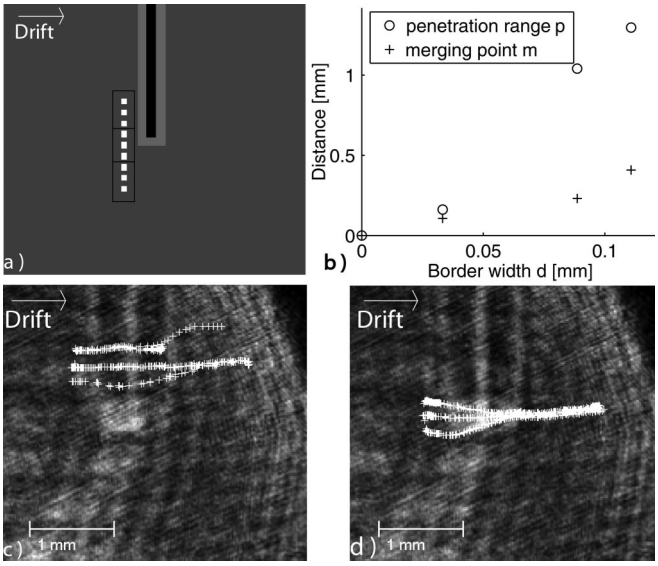

FIG. 8. (a) Interaction scheme of a solitary structure with a single barrier. (b) The penetration range into the barrier (○) and the distance where the paths of different solitary structures merge (+) depend on the border width d of the barrier. (c) At $d = 0.11$ mm solitary structures colliding with the barrier can pass it. (d) At the edge of the barrier solitary structures from different positions are attracted to the same path.

but the border width d is varied ($d = 0$–0.11 mm). Nine addressing positions for solitary structures are placed at distances of 0.37 mm to each other. The central one is placed again at the horizontal position of the barrier edge. All solitary structures are ignited in sequence in order to avoid mutual interaction.

Solitary structures ignited in the upper block drift straight onto the barrier. When using a barrier without a border, they disappear during collision with the barrier. If the border width is increased, a delayed disappearance is observed until they are able to pass the barrier. The penetration range p depicts how far they can move into the dark domain and is plotted with respect to the border width d in Fig. 8(b). Because of diffraction during free space propagation in the feedback loop, and diffusion in the LCLV, the intensity in the dark domain changes depending on the border width. Therefore, bistability occurs and solitary structures can penetrate the barrier. Solitary structures with addressing positions in the middle block interact with the barrier edge, being deflected after a certain propagation distance. Independent of the ignition position, they are attracted to the same path [Fig. 8(d)]. Varying the border width results in a variation of the position where different trajectories can no longer be separated. This position is referred to as merging position m in the following and depicted with respect to the border width d in FIG. 8(b). Positive values of m indicate an earlier merging of the trajectories. An increase of m with an increasing border width is observed. Solitary structures in the third block are ignited at distances larger than 0.74 mm with respect to the edge and remain unaffected since they cannot interact with the barrier.

Knowing the interaction behavior of solitary structures with the barrier, it is possible to vary the blocking properties of the barrier according to the desired behavior. By increasing the barrier width, solitary structures can propagate through the barrier. In the same way, the interaction range for the position-selective gap [Fig. 7(b)] can be controlled. By increasing d, solitary structures are attracted in a wider area to the gap and are able to pass it, but behind the gap the width where solitary structures exist is unchanged.

In conclusion, we have demonstrated experimental control of drifting solitary structures by using an incoherent external amplitude control in a unique way. Different control geometries are studied, which can be easily created, and yield versatile and excellent influence on the motion of solitary structures. In particular, we have developed a method to control their drift velocity. Control, providing both a position-selective element and a guiding element, has been implemented and characterized. These robust and easy-to-implement control methods for drifting solitary structures are contributions of utmost relevance considering the suggested applications of solitary structures in the context of all-optical information processing schemes.

[1] *Dissipative Solitons*, edited by N. Akhmediev and A. Ankiewicz (Springer, Berlin, 2005).
[2] W. J. Firth and C. O. Weiss, Opt. Photonics News **2002**, 54 (2002).
[3] S. Barland *et al.*, Nature (London) **419**, 699 (2002).
[4] B. Schäpers *et al.*, Phys. Rev. Lett. **85**, 748 (2000).
[5] A. Schreiber, B. Thüring, and M. Kreuzer, Opt. Commun. **136**, 415 (1997).
[6] B. Schäpers, T. Ackemann, and W. Lange, Proc. SPIE Int. Soc. Opt. Eng. **4271**, 130 (2001).
[7] V. B. Taranenko, K. Staliunas, and C. O. Weiss, Phys. Rev. A **56**, 1582 (1997).
[8] P. L. Ramazza *et al.*, Chaos **13**, 335 (2003).
[9] B. Gütlich *et al.*, Chaos **13**, 239 (2003).
[10] L. Spinelli *et al.*, Phys. Rev. A **66**, 023817 (2002).
[11] U. Bortolozzo and S. Residori, Phys. Rev. Lett. **96**, 037801 (2006).
[12] B. Gütlich *et al.*, Appl. Phys. B **81**, 927 (2005).
[13] B. Gütlich *et al.*, Chaos **17**, 037113 (2007).
[14] F. Pedaci *et al.*, Appl. Phys. Lett. **89**, 221111 (2006).
[15] R. Neubecker *et al.*, Phys. Rev. A **52**, 791 (1995).